Physics of the Earth and Planetary Interiors, 15 (1977) 90–106

PYROXENE–GARNET SOLID-SOLUTION EQUILIBRIA IN THE SYSTEMS $Mg_4Si_4O_{12}$–$Mg_3Al_2Si_3O_{12}$ AND $Fe_4Si_4O_{12}$–$Fe_3Al_2Si_3O_{12}$ AT HIGH PRESSURES AND TEMPERATURES

M. AKAOGI and S. AKIMOTO

Institute for Solid State Physics, University of Tokyo, Tokyo 106 (Japan) *

(Received March 22, 1977; accepted for publication April 6, 1977)

Akaogi, M. and Akimoto, S., 1977. Pyroxene–garnet solid-solution equilibria in the systems $Mg_4Si_4O_{12}$–$Mg_3Al_2Si_3O_{12}$ and $Fe_4Si_4O_{12}$–$Fe_3Al_2Si_3O_{12}$ at high pressures and temperatures. Phys. Earth Planet. Inter., 15: 90–106.

Pyroxene–garnet solid-solution equilibria have been studied in the pressure range 41–200 kbar and over the temperature range 850–1,450°C for the system $Mg_4Si_4O_{12}$–$Mg_3Al_2Si_3O_{12}$, and in the pressure range 30–105 kbar and over the temperature range 1,000–1,300°C for the system $Fe_4Si_4O_{12}$–$Fe_3Al_2Si_3O_{12}$. At 1,000°C, the solid solubility of enstatite ($MgSiO_3$) in pyrope ($Mg_3Al_2Si_3O_{12}$) increases gradually to 140 kbar and then increases suddenly in the pressure range 140–175 kbar, resulting in the formation of a homogeneous garnet with composition $Mg_3(Al_{0.8}Mg_{0.6}Si_{0.6})Si_3O_{12}$. In the $MgSiO_3$-rich field, the three-phase assemblage of β- or γ-Mg_2SiO_4, stishovite and a garnet solid solution is stable at pressures above 175 kbar at 1,000°C. The system $Fe_4Si_4O_{12}$–$Fe_3Al_2Si_3O_{12}$ shows a similar trend of high-pressure transformations: the maximum solubility of ferrosilite ($FeSiO_3$) in almandine ($Fe_3Al_2Si_3O_{12}$) forming a homogeneous garnet solid solution is 40 mol% at 93 kbar and 1,000°C.

If a pyrolite mantle is assumed, from the present results, the following transformation scheme is suggested for the pyroxene–garnet assemblage in the mantle. Pyroxenes begin to react with the already present pyrope-rich garnet at depths around 150 km. Although the pyroxene–garnet transformation is spread over more than 400 km in depth, the most effective transition to a complex garnet solid solution takes place at depths between 450 and 540 km. The complex garnet solid solution is expected to be stable at depths between 540 and 590 km. At greater depths, it will decompose to a mixture of modified spinel or spinel, stishovite and garnet solid solutions with smaller amounts of a pyroxene component in solution.

1. Introduction

It is widely believed that pyroxenes are the second most abundant group of minerals in the earth's upper mantle next to olivines. High-pressure transformations of pyroxenes to the denser structures are accepted as being partly responsible for the rapid increase in seismic wave velocity in the transition zone at a depth between about 400 and 1,000 km. Laboratory experiments on the high-pressure transformations of pyroxenes have been carried out extensively in the past decade by many investigators. In the system $FeSiO_3$–$MgSiO_3$, disproportionation of $(Fe,Mg)SiO_3$ clinopyroxene into $(Fe,Mg)_2SiO_4$ spinel or modified spinel plus stishovite was established in the pressure range up to about 200 kbar at 1,000°C (Ringwood and Major, 1966, 1968a; Akimoto and Syono, 1970; Ito et al., 1972). Recently, at higher pressures, recombination into ilmenite phase was reported for the Mg-rich side of the $MgSiO_3$–$FeSiO_3$ system (Kawai et al., 1974; Liu, 1976a, b). Further, at 250–300 kbar and at temperatures above 1,000°C, successful synthesis of a Mg-rich $(Mg,Fe)SiO_3$ perovskite has been announced by Liu (1974, 1975, 1976a, b) and Ito (1977a). Liu (1976b) also assigned the most abundant phase of $MgSiO_3$ observed by Ming and Bassett (1975) at about 250 kbar and 1,500°C as a perovskite phase.

* Address: Institute for Solid State Physics, University of Tokyo, Roppongi, Minato-ku, Tokyo 106, Japan.

Ringwood and Major (1966) and Ringwood (1967, 1970) investigated the solid solubility of pyroxenes in garnet structures at high pressures and temperatures. They reported that a series of aluminous pyroxene glasses with compositions of $MgSiO_3 \cdot 7\%Al_2O_3$ (wt.%) to $MgSiO_3 \cdot 13.5\%Al_2O_3$ and of $CaMgSi_2O_6 \cdot 10\%Al_2O_3$ and of $FeSiO_3 \cdot 10\%Al_2O_3$ crystallized into homogeneous garnet phases at pressures above approximately 100 kbar at about 1,000°C. The approximate composition of this type of garnet is expressed by the structural formula $M_3^{VIII}(AlM_{0.5}Si_{0.5})^{VI}Si_3^{IV}O_{12}$, M = Mg, Fe^{2+}, Ca, where the superscripts denote the coordination of the specified cation by oxygen. Natural occurrence of garnet having a composition corresponding to bronzite was reported in a shocked meteorite by Smith and Mason (1970). Ringwood (1970, 1975) suggested, on the basis of these experimental results and natural observations, that at greater depths in the mantle pyroxenes transform first to the garnet structure in the presence of some amount of Al_2O_3, Cr_2O_3 and Fe_2O_3, rather than to the mixed phase of spinel or modified spinel plus stishovite.

In view of the fact that in the previous investigations in Ringwood's laboratory (Ringwood and Major, 1966; Ringwood, 1967, 1970) the garnet solid solutions could be prepared only by devitrifying glasses during the short run time, there remained a possibility that they might be metastable. Further, Ringwood and Major were unsuccessful in the direct measurement of run temperature at high pressures above 100 kbar because of the apparatus limitations. In a Bridgman anvil used by Ringwood and Major (1968b), the run temperatures were estimated by some indirect methods, and the possible error in individual runs amounted to ±200°C. Some uncertainties in the pressure determination were also inherent in the Bridgman anvil apparatus, especially in the pressure range above 150 kbar, because of the lack of a reliable pressure calibration method. All these ambiguities made the previous data on the pyroxene–garnet transformation inevitably qualitative rather than quantitative. Further comprehensive investigations are required in order to make the pyroxene–garnet transformation applicable to geophysical problems relating to the mantle transition zone.

Very recently, new types of high-pressure apparatus capable of generating pressures up to 250 kbar at high temperatures (1,000–1,500°C) for extended periods were developed in our laboratory (Yagi and Akimoto, 1976a; Akimoto et al., 1977; Kawada, 1977). Pressure values in these apparatus can be determined accurately on the basis of the compression of NaCl (Yagi and Akimoto, 1976a, b; Akimoto et al., 1977). Using these modern high-pressure techniques, the pyroxene–garnet transformation in the mantle is re-examined in the present investigation. It is attempted to determine the detailed transformation diagram of the enstatite–pyrope system, $Mg_4Si_4O_{12}$–$Mg_3Al_2Si_3O_{12}$, as well as the ferrosilite–almandine system, $Fe_4Si_4O_{12}$–$Fe_3Al_2Si_3O_{12}$, over a wide range of pressure and temperature up to 200 kbar and 1,300°C. Special caution is paid to the starting materials in the high-pressure experiments in order to reach the final conclusion on the possible metastability of the garnet solid solutions reported by Ringwood (1967, 1970). The present expanded knowledge of the pyroxene–garnet transformation is combined with the latest seismic wave velocity model in the mantle. The role of the phase transformations of pyroxenes in the formation of the mantle transition zone is discussed.

2. Experimental procedure

2.1. High-pressure and high-temperature technique

Phase-equilibrium experiments in the present study were made using three types of high-pressure apparatus – a tetrahedral-anvil type, a cubic-anvil type and a new double-staged cubic-octahedral-anvil type. In the experiments in the system $Mg_4Si_4O_{12}$–$Mg_3Al_2Si_3O_{12}$, the cubic-octahedral-anvil-type high-pressure apparatus was used in the runs of the pressure range from 80 to 200 kbar, and the tetrahedral-anvil-type apparatus was used for pressures below 80 kbar. Runs in the system $Fe_4Si_4O_{12}$–$Fe_3Al_2Si_3O_{12}$ were made using the cubic-anvil-type apparatus in the pressure range from 90 to 105 kbar and using the tetrahedral-anvil-type apparatus in the range from 30 to 93 kbar.

The double-staged cubic-octahedral-anvil-type apparatus used in this study is principally similar to a split-sphere apparatus described by Kawai and Endo (1970). We used a split-cylinder made of hardened steel as the first-stage cubic-anvil system. The second-stage anvil assembly driven by the outer cubic-anvil system is

composed of eight tungsten-carbide cubes with an edge length of 20.5 mm. One corner of each cube is truncated to form a regular triangle. A regular octahedron is enclosed by eight triangles at the center of the second-stage anvil assembly. An octahedron of semi-sintered polycrystalline MgO was used as a pressure-transmitting medium. The use of the MgO pressure medium is based on the recent observation of the temperature effect on the pressure-generating efficiency of the conventional pyrophyllite pressure cell. High-pressure and high-temperature X-ray diffraction studies have revealed that disproportionation of pyrophyllite around the furnace space to the denser minerals, such as stishovite plus kyanite, results in a remarkable decrease of pressure acting on the sample within the furnace (Inoue, 1975; Akimoto et al., 1977). In order to avoid this inconvenience of the pyrophyllite cell, we adopted the polycrystalline MgO cell exclusively in the double-staged cubic-octahedral-anvil apparatus which was generally used at the stable field of stishovite.

Preformed gaskets, made of the mixture of asbestos, sodium chloride, hematite and amorphous boron in the ratio of 4:4:1:1 by weight, were used in the second-stage octahedral-anvil system. Thin bakelite sheets were placed between six outer steel anvils and eight inner tungsten-carbide anvils for electrical insulation. The double-staged cubic-octahedral-anvil system covered by a cylindrical thick rubber shell was immersed into an oil reservoir. With rising oil pressure, the whole cylindrical assemblage shrank and a very high pressure was generated in the central octahedron in which the sample was charged. A more detailed description of the present cubic-octahedral-anvil apparatus is given in a separate paper (Kawada, 1977).

Two different sizes of inner tungsten-carbide anvils were used, depending on the maximum pressure desired. Anvils with a triangular-edge length of 2.5 mm were used with a 7-mm-edge MgO octahedron for most runs in the range from 80 to 150 kbar. A combination of 1.8-mm-edge anvils with a 6-mm-edge MgO octahedron was adopted chiefly for runs from 150 to 200 kbar.

The furnace assembly used for the cubic-octahedral press is illustrated in Fig.1. In the runs with 2.5-mm-edge anvils, a graphite tube, 4.0 mm long, with outer diameter 1.2 mm and 0.8 mm inner diameter, bounded by 1.0 mm long graphite end plugs, was used for heating the samples. Electrical power was supplied to

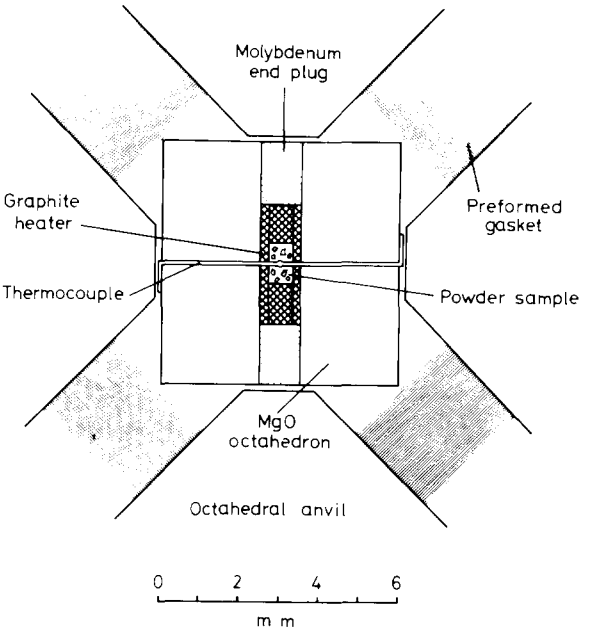

Fig.1. Furnace assembly used in conjunction with 1.8-mm-edge inner diameter anvils of a double-staged cubic-octahedral-anvil type of high-pressure apparatus.

the furnace through 50 μm thick gold current leads which make contact with the faces of a pair of opposite anvils. Smaller graphite tubes, 3.0 mm long, with outer diameter 1.0 mm and 0.6 mm inner diameter, with graphite end plugs, 1.0 mm long, were used for the runs with 1.8-mm-edge anvils. In this case a molybdenum disk was used as the current lead.

Powder samples were directly put into the graphite furnace. Temperatures were measured with a Pt/Pt–13%Rh thermocouple, 0.1 mm in diameter. The hot junction was placed in the central part of the sample. Thermocouple leads from the hot junction were brought out to the faces of a pair of opposite anvils. The run temperatures were corrected for the increase of the surface temperature of the inner anvils. Due to the relatively high thermal conductivity of MgO and the absence of a cooling system for the anvils, the temperature rise on the inner anvil surface was considerable, about 200°C when the temperature at the center of the furnace was 1,000°C. No correction was made for the effect of pressure on the thermoelectromotive force of the thermocouple.

The tetrahedral-anvil-type apparatus previously

described (Akimoto et al., 1965) was also used in the runs below 93 kbar. Two different sizes of tungsten-carbide anvils were used. Anvils 15 mm in edge in combination with a 20-mm-edge pyrophyllite tetrahedron were used. A tubular graphite furnace, 6.0 mm long, with outer diameter 3.0 mm and 2.0 mm inner diameter, was placed diagonally with the axis of the cylinder between opposite edges of the pyrophyllite tetrahedron. In the runs using 9-mm-edge anvils with a 14-mm-edge pyrophyllite tetrahedron, a smaller graphite tube, 3.5 mm long, with outer diameter 2.5 mm and 1.8 mm inner diameter, was adopted. Powder samples of the system $Mg_4Si_4O_{12}$–$Mg_3Al_2Si_3O_{12}$ were embedded directly into the central part, 1.0–2.0 mm in thickness, of the graphite furnace. A pair of pyrophyllite disks were placed at both ends of the sample in order to reduce the temperature gradient within the furnace. A pair of thin boron-nitride disks were inserted between the sample and the pyrophyllite disk to prevent the reaction between them at high temperatures. In most runs in the system $Fe_4Si_4O_{12}$–$Fe_3Al_2Si_3O_{12}$ the powder sample was enclosed into a gold capsule which was placed in the central part of the graphite furnace in order to avoid the reduction of ferrous iron at high temperatures. Temperatures were measured with a Pt/Pt–13%Rh thermocouple, 0.1–0.2 mm in diameter. The hot junction was placed in the center of the sample or in close contact with the capsule.

The cubic-anvil type of the high-pressure apparatus was used in most runs in the pressure range from 90 to 105 kbar in the system $Fe_4Si_4O_{12}$–$Fe_3Al_2Si_3O_{12}$. 3-mm-edge tungsten-carbide anvils with a 5-mm-edge pyrophyllite cube were used. A graphite tube heater, 2.4 mm long, outer diameter 2.0 mm and inner diameter 1.5 mm was placed at the center of the pyrophyllite cube with the axis of the cylinder perpendicular to the opposite faces of the cube. Powder samples were enclosed into a gold capsule in the central part of the graphite furnace. The determination of run temperatures was again made by a Pt/Pt–13%Rh thermocouple, 0.1 mm in diameter.

Pressure values in these multi-anvil apparatus were calibrated against press load at room temperature by means of several pressure-fixed points. Below 100 kbar, the well-established fixed points of low-Bi (25.5 kbar), low-Ba (55 kbar), high-Bi (77 kbar) and Sn (100 kbar) were used. The latest data in our laboratory on the transformation pressure of high-Ba (126 kbar), Pb (142 kbar), ZnS (162 kbar) and GaAs (193 kbar) were also adopted as fixed points between 100 and 200 kbar (Akimoto et al., 1975; Yagi and Akimoto, 1976b, 1977). In the double-staged cubic-octahedral-anvil apparatus, the semiconductor–metal transitions in ZnS and GaAs were found to be reproducible within an accuracy of ±2%.

Recent in-situ X-ray diffraction measurements strongly indicate that some corrections are required for the pressure values calibrated at room temperature when the multi-anvil apparatus was used for high-temperature work (Inoue, 1975; Yagi and Akimoto, 1976a; Akimoto et al., 1977). The phase boundary curves between coesite and stishovite:

$$P\,(\text{kbar}) = 80 + 0.011\ T\,(^\circ\text{C})$$

(Yagi and Akimoto, 1976a), and between pyroxene and ilmenite in $ZnSiO_3$:

$$P\,(\text{kbar}) = 91 + 0.02\ T\,(^\circ\text{C})$$

(Akimoto et al., 1977), which were determined on the basis of the compression of NaCl at high temperature, were used for this purpose. A high-temperature correction was found to amount to approximately +7% for the semi-sintered MgO pressure medium and to −5% at most for the pyrophyllite pressure cell in the pressure range 90–120 kbar at temperatures 1,000–1,400°C.

2.2. Starting materials

In the experiments in the system $Mg_4Si_4O_{12}$–$Mg_3Al_2Si_3O_{12}$, three types of starting materials were used: (1) homogeneous glass; (2) a mixture of MgO, silicic acid and alumina gel in the desired proportion; and (3) a mixture of synthetic clinoenstatite and pyrope. In most runs starting material (1) was used. Starting materials (2) and (3) were used in auxiliary runs.

Glasses of nominal compositions 5, 20, 40, 50, 60, 75 and 100 mol% of $Mg_4Si_4O_{12}$ in the system $Mg_4Si_4O_{12}$–$Mg_3Al_2Si_3O_{12}$ were prepared by Dr. H. Takei, Tohoku University. These glasses were examined by an optical microscope and by an electron microprobe analyser. Less than 1% of quench crystal (probably forsterite) was contained in each glass. Microprobe analyses indicated that these glasses were almost homogeneous and chemical compositions determined

were 5.4, 17.7, 40.6, 47.7, 59.3, 73.7 and 100.0 mol% of $Mg_4Si_4O_{12}$ in the system $Mg_4Si_4O_{12}$–$Mg_3Al_2Si_3O_{12}$, respectively. The glasses were ground into a fine powder and used as starting materials. Mineralizers such as H_2O were not added to the glasses. Clinoenstatite was prepared by devitrifying $MgSiO_3$ glass at 1,200°C at atmospheric pressure. Pyrope was synthesized from the mixture of brucite, silicic acid and corundum at 37 kbar and about 1,000°C. Both of these crystals were well crystallized into single-phase material. Intimate powder mixtures of clinoenstatite and pyrope thus obtained in the desired proportion were used as a starting material. In the runs of pure $Mg_4Si_4O_{12}$ composition, clinoenstatite and $MgSiO_3$ glass were used.

In the runs in the system $Fe_4Si_4O_{12}$–$Fe_3Al_2Si_3O_{12}$, three types of starting materials were used: (1) a mixture of fayalite, silicic acid and aluminum hydroxide; (2) a mixture of clinoferrosilite and almandine; and (3) orthoferrosilite. In most runs starting material (1) was used. Fayalite was prepared by the method of Akimoto and Fujisawa (1965). Clinoferrosilite and orthoferrosilite were synthesized from a mixture of fayalite and amorphous anhydrous silica at 1,000°C at 70 and 40 kbar, respectively. Almandine was synthesized from a mixture of fayalite, corundum and amorphous anhydrous silica in the desired proportion at 30 kbar and 1,150°C. Intimate powder mixtures of clinoferrosilite and almandine thus obtained in the desired proportion, containing no H_2O, were used as a starting material. Starting material (3) was used only for the runs of pure $Fe_4Si_4O_{12}$ composition.

2.3. Determination of pyroxene–garnet solid-solution equilibria

The experimental method used in determining the equilibrium diagrams was a conventional quenching technique. The sample was held at a desired pressure–temperature condition for a time interval sufficient for equilibrium, and was quenched isobarically to room temperature by turning off the heating power. A few auxiliary runs, in which homogeneous garnet solid solution was used as the starting material, were made to examine whether the pyroxene–garnet equilibria were reached in the present experimental conditions. After the run, all the quenched samples were examined under the microscope and by X-ray powder diffraction.

Cell parameters of the garnet solid solution in the run products were determined by means of the X-ray powder diffractometer. Nine diffraction lines of garnet: (642), (640), (444), (611), (521), (431), (422), (332) and (420) were generally used. As described in the following section, lattice parameters refined by the least-squares method were used for estimating the chemical composition of the garnet solid solution. For the purpose of determining the Al_2O_3 contents in the aluminous orthoenstatite coexisting with the garnet solid solution, the d-spacing of the (060) diffraction line was used, because the b-edge length of orthoenstatite is most sensitive to Al_2O_3 contents. From the observed d-spacing of the (060) reflection, Al_2O_3 contents were calculated using the relationship between b-edge length and composition reported by Skinner and Boyd (1964). In the determination of cell parameters of garnet and d-spacings of (060) of orthopyroxene, the goniometer scanning speed was selected as 0.5° (2θ) per minute. Calibration of the goniometer was made using a high-purity silicon sample as an external standard. Iron K_{α_1} radiation was used throughout.

Chemical compositions of the garnet solid solution in several run products were determined by means of the electron-microprobe analyser. Analytical procedures are similar to those reported by Nakamura and Kushiro (1970). Correction methods are the same as those described by Bence and Albee (1968).

3. Results and discussion

3.1. The system $Mg_4Si_4O_{12}$–$Mg_3Al_2Si_3O_{12}$

Experimental results in the system $Mg_4Si_4O_{12}$–$Mg_3Al_2Si_3O_{12}$ are summarized in Table I. Regarding the end-member $Mg_4Si_4O_{12}$, it is confirmed that the clinoenstatite phase of $MgSiO_3$ disproportionates into modified spinel (β) plus stishovite without the intervention of any intermediate phase such as garnet. The pressure for the disproportionation was determined to be 175 kbar at 1,000°C. This transition pressure is just the same as that determined by Ito (1977b) and that proposed by Liu (1976b). The obtained phase relations for $MgSiO_3$ are shown in a pressure–temperature diagram (Fig.2). The boundary curve has a positive slope and is determined to be:

$$P\,(\text{kbar}) = 145 + 0.03\,T\,(^\circ\text{C})$$

TABLE I

Results of high-pressure high-temperature experiments in the system $Mg_4Si_4O_{12}$–$Mg_3Al_2Si_3O_{12}$

Run No.	Composition ($Mg_4Si_4O_{12}$ mol%)	Pressure (kbar)	Time (min)	Phases present	Lattice parameter of garnet solid solution (Å)
Temperature 850°C:					
0921	41	150	90	Gar + Cpx (tr.)	11.464(1)
0920	41	160	120	Gar	11.467(1)
Temperature 1,000°C:					
07251	5	41	120	Gar + Opx (tr.)	11.457(1)
07252	5	68	120	Gar	11.459(1)
0622	5	84	60	Gar	11.459(1)
06162	18	68	120	Gar + Opx	11.460(1)
0521	18	106	45	Gar + Opx	11.462(1)
0714	18	114	60	Gar	11.461(1)
0501	18	123	60	Gar	11.463(1)
06161	41	41	120	Gar + Opx	11.458(1)
0603	41	68	180	Gar + Opx	11.460(1)
0709	41	94	60	Gar + Cpx	11.461(1)
0517	41	106	60	Gar + Cpx	11.460(1)
0502	41	123	30	Gar + Cpx	11.464(1)
0723	41	137	60	Gar + Cpx	11.464(1)
0828	41	140	60	Gar + Cpx	11.464(1)
0506	41	150	60	Gar + Cpx (tr.)	11.465(1)
0918	41	160	60	Gar + Cpx (tr.)	11.464(1)
1123	41	180	30	Gar	11.465(1)
06291	48	68	180	Gar + Opx	11.459(1)
06292	48	106	90	Gar + Cpx	
0630	48	123	90	Gar + Cpx	
0922	48	174	60	Gar + Cpx (tr.)	
1028	48	186	90	Gar	11.469(1)
1026	48	200	90	Gar + St + β + γ	11.469(1)
1021	59	170	60	Gar + Cpx	11.468(1)
1020	59	180	65	Gar + St + β	11.472(1)
0615	74	68	120	Gar + Opx	11.459(1)
0529	74	106	60	Cpx + Gar	11.460(1)
0710	74	142	60	Gar + Cpx	11.473(1)
0813	74	167	60	Gar + Cpx	11.473(1)
1016	74	190	120	Gar + St + β + Cpx	11.471(2)
0706	100	132	60	Cpx	
0709	100	143	35	Cpx	
1014*	100	172	120	Cpx	
1012*	100	180	60	Cpx + St + β	
1015*	100	190	120	Cpx + St + β + γ (tr.)	
Temperature 1,200°C:					
0522	41	68	60	Gar + Opx	11.460(1)
0821	41	146	7	Gar + Cpx	11.462(1)
0823	41	157	20	Gar + Cpx	11.463(1)
0824	41	167	30	Gar	11.464(1)
1025	48	200	30	Gar	11.470(1)
1115*	100	179	45	Cpx	
1116*	100	190	60	Cpx + β + St	
Temperature 1,300°C:					
1122*	100	187	20	Cpx + St + β	
1118*	100	195	10	Cpx + St + β	

Gar = garnet solid solution; Opx = orthopyroxene solid solution; Cpx = clinopyroxene solid solution; β = modified spinel; γ = spinel; St = stishovite; tr. = trace.

*Starting material is clinoenstatite. In all other runs glasses in the system $Mg_4Si_4O_{12}$–$Mg_3Al_2Si_3O_{12}$ are used.

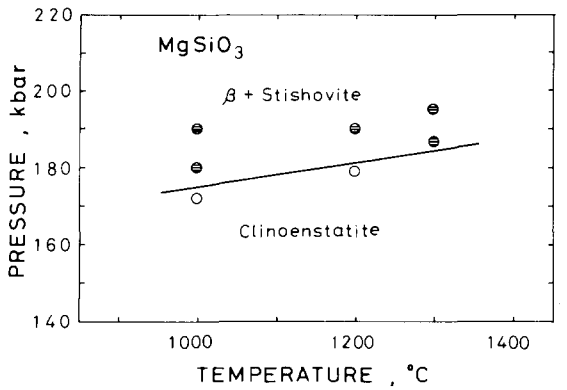

Fig. 2. Pressure–temperature stability diagram for the disproportionation of clinoenstatite, $MgSiO_3$. β = modified spinel.

Phase relationships in the system $Mg_4Si_4O_{12}$–$Mg_3Al_2Si_3O_{12}$ in the pressure range from 41 to 200 kbar at 1,000°C are shown in Fig. 3, which shows the single-phase field of garnet solid solutions, the two-phase field of pyroxene solid solutions plus garnet solid solutions, and the three-phase field of modified

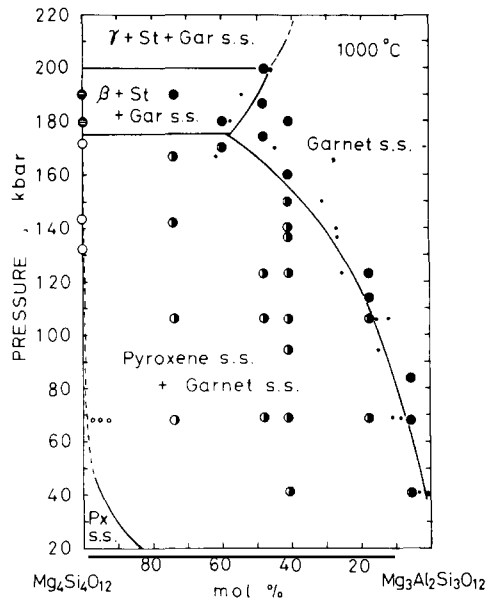

Fig. 3. Phase relationships in the system $Mg_4Si_4O_{12}$–$Mg_3Al_2Si_3O_{12}$ at pressures up to 200 kbar and at 1000°C. Px = pyroxene; Gar = garnet; St = stishovite; β = modified spinel; γ = spinel.
Solid dots along the garnet solvus indicate the garnet composition estimated from the lattice parameter. *Open dots* along the pyroxene solvus indicate the pyroxene composition estimated from the d_{060}-spacing.

spinel (β) plus stishovite plus garnet solid solutions. Lattice parameters of garnet solid solutions in the two- and three-phase fields were determined and used for estimating the boundary of the garnet field. These are shown as solid dots in Fig. 3. At pressures below 50 kbar, the stability field of aluminous orthoenstatite was investigated by Boyd and England (1964) and MacGregor (1974). MacGregor's recent result on the pyroxene solvus was shown in Fig. 3. The phase boundary between the field of modified spinel (β) plus stishovite plus garnet solid solutions and that of spinel (γ) plus stishovite plus garnet solid solutions is found to be consistent with an independent determination of the transformation pressure from modified spinel to spinel in Mg_2SiO_4 (Kawada, 1977). In the present experiments, orthopyroxene coexisting with garnet solid solution transformed to clinopyroxene at pressures around 100 kbar and at 1,000°C. Since the transformation is known to be greatly affected by the presence of shear stress, the phase boundary between orthopyroxene and clinopyroxene is disregarded in Fig. 3.

At a fixed composition, the relative concentration of garnet to pyroxene solid solutions was found to increase systematically with increasing pressure. In Table I a general trend of an increase in the lattice parameter of the garnet solid solution with increasing pressure is also seen. These experimental results indicate the existence of a broad two-phase region, where garnet solid solutions are coexisting with pyroxene solid solutions. At 1,000°C, the solubility of $Mg_4Si_4O_{12}$ component in the homogeneous garnet solid solution increased with increasing pressure up to 175 kbar which corresponds to the disproportionation pressure of clinoenstatite into modified spinel plus stishovite. Above that pressure the solubility diminished. The composition within the garnet solid solution containing the highest $Mg_4Si_4O_{12}$ component is about $[Mg_4Si_4O_{12}]_{0.6}[Mg_3Al_2Si_3O_{12}]_{0.4}$. Fig. 3 shows that, at the composition of 60%$[Mg_4Si_4O_{12}]$ · 40%$[Mg_3Al_2Si_3O_{12}]$ (mol%), the relative concentration of garnet solid solution to pyroxene solid solution increases gradually from about 40 to 140 kbar, and then increases rather rapidly up to 175 kbar, where an almost single-phase garnet solid solution appears. Above 175 kbar the garnet solid solution decomposes into a mixture of modified spinel, stishovite and garnet solid solution containing less than 60 mol%

TABLE II

Chemical composition and lattice parameter of homogeneous garnet solid solutions synthesized at 1,000°C

Run No.	0714	0622	142	Run No.	0714	0622	142
Pressure (kbar)	114	84	88	Pressure (kbar)	114	84	88
Composition (wt.%):				*Atomic ratio (12 oxygens):*			
MgO	31.10	29.98	–	Mg	3.148	3.029	–
FeO	–	–	44.45	Fe	–	–	3.183
Al_2O_3	20.39	23.43	16.97	Al	1.632	1.872	1.713
SiO_2	47.15	45.45	36.48	Si	3.202	3.081	3.124
Total	98.64	98.86	97.90	Total	7.982	7.982	8.020
Composition (mol%):							
$Mg_4Si_4O_{12}$	17.7	6.2	–				
$Mg_3Al_2Si_3O_{12}$	82.3	93.8	–				
$Fe_4Si_4O_{12}$	–	–	15.2				
$Fe_3Al_2Si_3O_{12}$	–	–	84.8				
Lattice parameter (Å):	11.461(1)	11.459(1)	11.536(1)				

$Mg_4Si_4O_{12}$. Although these results support qualitatively Ringwood's (1967) idea of the pyroxene–garnet transformation in the system $Mg_4Si_4O_{12}$–$Mg_3Al_2Si_3O_{12}$, some quantitative disagreements were found between these two investigations. He found that the rapid increase in the proportion of garnet solid solution took place at pressures from 90 to 110 kbar for the composition of $MgSiO_3 \cdot 10\%Al_2O_3$ (wt.%), corresponding to $60\%[Mg_4Si_4O_{12}] \cdot 40\%[Mg_3Al_2Si_3O_{12}]$ (mol%). The discrepancy may be due to the difference in run time and run temperature. In Ringwood's experiments, run times were limited to about 5 min at temperatures estimated to be approximately 900°C. On the other hand, run times in the present study were much longer, 1–3 h at 1,000°C, and are more likely to approach the equilibrium state.

Chemical compositions of the homogeneous garnet solid solutions were determined by an electron microprobe analyser to examine whether or not these garnets maintain the compositions of the starting materials. Results for two run products are shown in Table II, together with the lattice parameters. Although a slight excess of Si compared with Mg, inherited from the starting glass compositions, was observed, the determined compositions are almost identical with those of the starting glasses and are on the join of $Mg_4Si_4O_{12}$–$Mg_3Al_2Si_3O_{12}$. Based on this information, the lattice parameters of the homogeneous garnet solid solutions were plotted against compositions of the starting glass in Fig.4. It is shown in the figure that the lattice parameter increases linearly with increasing amount of $Mg_4Si_4O_{12}$ from 11.457(1) Å for $Mg_3Al_2Si_3O_{12}$ pyrope. The cell parameter of pyrope obtained in this study is in good agreement with the 11.456(2) Å of Boyd and England (1959) and 11.459(1) Å of Skinner (1956). The lattice parameter for $[Mg_4Si_4O_{12}]_{0.6}$-$[Mg_3Al_2Si_3O_{12}]_{0.4}$ garnet is estimated from the

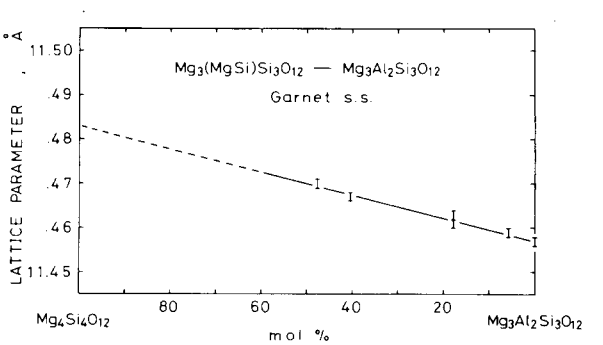

Fig. 4. Lattice parameter vs. composition of the homogeneous $Mg_4Si_4O_{12}$-$Mg_3Al_2Si_3O_{12}$ garnet solid solutions.

figure to be 11.473 Å, which is in reasonable agreement with the value of 11.477 Å obtained for the same composition by Ringwood (1967). For the virtual garnet end-member, $Mg_4Si_4O_{12}$, the lattice parameter of 11.483 Å is obtained by extrapolation. The calculated density of the virtual $Mg_4Si_4O_{12}$ garnet so estimated is 3.52 g/cm^3, which is 9.7% larger than that of clinoenstatite and is 4.5% smaller than that of the mixture of modified spinel and stishovite with the same composition.

All these garnet solid solutions synthesized with compositions from $Mg_3Al_2Si_3O_{12}$ to $[Mg_4Si_4O_{12}]_{0.6}$-$[Mg_3Al_2Si_3O_{12}]_{0.4}$ have a cubic symmetry and are optically isotropic. The refractive index of the homogeneous garnet solid solution, $[Mg_4Si_4O_{12}]_{0.48}$-$[Mg_3Al_2Si_3O_{12}]_{0.52}$ was determined to be 1.708(2) by the immersion method. This value is a little smaller than the refractive index of the pure pyrope synthesized in the present study, 1.712(2). This slight decrease of the refractive index towards the $Mg_4Si_4O_{12}$-rich side is consistent with the density change in the $Mg_4Si_4O_{12}$–$Mg_3Al_2Si_3O_{12}$ garnet solid-solution system; the density of pure pyrope, 3.56 g/cm^3, is 1.1% larger than that of the virtual $Mg_4Si_4O_{12}$ garnet.

It must be noted here that homogeneous garnet solid solutions in Fig.3 were all crystallized from the starting material of glasses at 1,000°C. Since this temperature is far below the solidus, the possibility of nucleating metastable garnet solid solutions should be considered. This problem has already been pointed out in the previous studies of Ringwood and Major (1966) and Ringwood (1967). To examine whether these garnet solid solutions are stable phases or not, and whether or not the garnet solid-solution solvus in Fig.3 represents a real equilibrium boundary, three approaches were made. The first examination was made by comparing the experimental results obtained at a specific pressure–temperature condition from glasses with different chemical composition. The experimental results of runs in the two-phase region at 68 kbar and 1,000°C with different starting glasses were rearranged in Table III. In this table the compositions of the garnet solid solutions were estimated from the relationship between lattice parameter and composition shown in Fig.4, and those of the orthopyroxene solid solutions were calculated from the observed d_{060}-spacing using the relationship between b-edge length and composition determined by Skinner and Boyd (1964). These compositions are shown by solid and open dots in Fig.3. Although slight scattering of the compositional data for the orthopyroxene solid solution was found, the compositions of the garnet solid solutions synthesized at 68 kbar and 1,000°C from the four different starting glasses with composition of 18, 41, 48 and 74 mol% $Mg_4Si_4O_{12}$ are in good agreement with each other. These results may suggest that the garnet solid-solution boundary in Fig.3 approximately represents a real equilibrium boundary.

Secondly, the synthesis of the garnet solid solutions from the non-glassy starting materials was attempted. The garnet solid solutions were prepared in the two-phase region at 68 kbar and at temperatures ranging from 1,000 to 1,450°C by reacting mixtures of the component oxides or mixtures of pure pyrope and clinoenstatite for 1–5 h. The results are compared in

TABLE III

Compositions of coexisting garnet and orthopyroxene solid solutions at 68 kbar and 1,000°C

Run No.	Starting-material composition ($Mg_4Si_4O_{12}$ mol%)	Pressure (kbar)	Garnet solid solution		Orthopyroxene solid solution	
			lattice parameter (Å)	composition (mol%)	d_{060}-spacing (Å)	composition (mol%)
06162	18	68	11.460(1)	11	1.4661	92
0603	41	68	11.460(1)	11	1.4672	95
1108*	41	68	11.460(1)	11	1.4661	92
06291	48	68	11.459(1)	8	1.4681	97
0615	74	68	11.459(1)	8	1.4671	94

*Starting material is a mixture of oxides. In all other runs glasses are used.

TABLE IV

Comparison of the run products at 68 kbar using different kinds of starting materials with the composition of 41%[$Mg_4Si_4O_{12}$] · 59%[$Mg_3Al_2Si_3O_{12}$] (mol%)

Run No.	Starting material	Temperature (°C)	Time (h)	Garnet solid solution	
				lattice parameter*[1] (Å)	composition ($Mg_4Si_4O_{12}$ mol%)
0603	glass	1,000	3	11.460(1)	11
1108	mixture of oxides	1,000	5	11.460(1)	11
0522	glass	1,250	1	11.460(1)	11
1104	mixture of oxides	1,250	3	11.461(1)	15
1109	glass	1,450	1	11.460(1)	11
1114	pyrope + clinoenstatite	1,450	5	11.461(1)	15
1103*[2]	garnet solid solution	1,450	5	11.463(1)	22

*[1] Lattice parameter for pyrope, $Mg_3Al_2Si_3O_{12}$: a = 11.457(1) Å.
*[2] The reverse reaction with the starting material of homogeneous garnet solid solution.
Phases present in the run products are garnet solid solution and ortho- or clinopyroxene solid solution.

Table IV with those obtained by devitrifying glasses. The lattice parameters of the garnets crystallized from a mixture of oxides (MgO, silicic acid and alumina gel), and from the mixture of pyrope and clinoenstatite were larger than that of pyrope by an amount greater than the experimental error and are in good agreement with those of the garnet from glass at 1,000, 1,250 and 1,450°C, respectively. The compositions of these garnets estimated from the cell parameters, using the empirical relationship shown in Fig.4, were 11–15 mol% in $Mg_4Si_4O_{12}$. From these results, it can be concluded that the garnet solid solution containing substantial amounts of the $Mg_4Si_4O_{12}$ component can be synthesized not only from glass but also from a mixture of oxides as well as from a mixture of end-member crystals.

The third and most definite examination was made through a reverse reaction using homogeneous garnet solid solution as a starting material. Single-phase garnet $[Mg_4Si_4O_{12}]_{0.41}-[Mg_3Al_2Si_3O_{12}]_{0.59}$, which had been synthesized above 160 kbar, was subjected to 68 kbar and 1,450°C for 5 h. The result is listed in Table IV. The most remarkable feature of the run product was an appearance of the pyroxene phase in addition to the garnet phase. It is noted that the pyroxene appearing in the run product takes the clinopyroxene structure. This is slightly inconsistent with the experimental results obtained at the same pressure–temperature condition by devitrifying homogeneous glass or by reacting a mixture of end-member crystals; in these runs pyroxene crystallized into the orthopyroxene structure. The inconsistency may be due to the shear stress which accompanies the exsolution of pyroxene from the homogeneous garnet solid solution in the reverse reaction. It was further revealed that the lattice parameter of the newly equilibrated garnet solid solution decreased considerably. The composition of the garnet solid solution estimated from the lattice parameter is 22 mol% in $Mg_4Si_4O_{12}$, which is much smaller than the 41 mol% of the starting garnet solid solution.

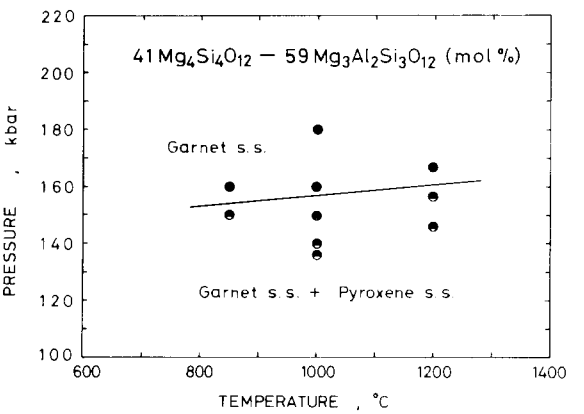

Fig. 5. Pressure–temperature stability diagram for forming the homogeneous garnet solid solution in 41%[$Mg_4Si_4O_{12}$] · 59%[$Mg_3Al_2Si_3O_{12}$] (mol%).

This result indicates that the reaction forming the garnet solid solution in the $Mg_4Si_4O_{12}$–$Mg_3Al_2Si_3O_{12}$ system is reversible. Judging from all these results in the three studies, it may confidently be concluded that the garnet solid solution obtained in the present study represents a thermodynamically stable phase.

The knowledge of the dP/dT gradient of the garnet solid-solution solvus is indispensable for applying the pyroxene–garnet transformation diagram to the problems relating to the seismic discontinuities in the mantle. Pressure values in which the pyroxene solid solution vanishes completely were determined as a function of temperature for the 41%[$Mg_4Si_4O_{12}$]·59%[$Mg_3Al_2Si_3O_{12}$] (mol%) composition. The results were shown in Table I and Fig.5. It is seen that the boundary possesses a positive and gentle slope. The boundary curve was tentatively determined as:

$$P\,(\text{kbar}) = 137 + 0.02\,T\,(^\circ\text{C})$$

3.2. *The system $Fe_4Si_4O_{12}$–$Fe_3Al_2Si_3O_{12}$*

Experimental results in the system $Fe_4Si_4O_{12}$–$Fe_3Al_2Si_3O_{12}$ are summarized in Table V. The phase

TABLE V

Results of high-pressure high-temperature experiments in the system $Fe_4Si_4O_{12}$–$Fe_3Al_2Si_3O_{12}$

Run No.	Composition ($Fe_4Si_4O_{12}$ mol%)	Pressure (kbar)	Time (min)	Phases present	Lattice parameter of garnet solid solution (Å)
Temperature 1000°C:					
063	6	64	180	Gar + Cpx (tr.)	
062	6	77	120	Gar	11.529(1)
143	14	75.5	90	Gar + Cpx	
144	14	85	120	Gar	
142	14	88	120	Gar	11.536(1)
202	20	95	180	Gar	11.541(1)
3010	30	93	180	Gar	
302	30	95	120	Gar	11.545(2)
303	30	105	120	Gar + Sp + St	
403	40	90	60	Gar + Cpx	
401	40	100	90	Gar + Sp + St	11.545(2)
603	60	90	180	Gar + Cpx	
605	60	100	60	Gar + Sp + St	
801	80	87	120	Cpx + Gar	
1001*[1]	100	88	20	Cpx	
1002*[1]	100	94	20	Sp + St	
Temperature 1200°C:					
308	30	93	90	Gar + Cpx (tr.)	
904*[2]	90	30	120	Opx + Gar (tr.)	
Temperature 1300°C:					
145*[3]	14	95	120	Gar	
203*[4]	20	60	120	Gar + Cpx (tr.)	
309*[4]	30	64	180	Gar + Cpx	11.540(1)

Gar = garnet solid solution; Cpx = clinopyroxene solid solution; Opx = orthopyroxene solid solution; Sp = spinel; St = stishovite; tr. = trace.

Starting material:

*[1] Orthoferrosilite.

*[2] Mixture of fayalite, α-quartz and corundum.

*[3] Mixture of clinoferrosilite and almandine.

*[4] Garnet solid solution for the reverse reaction.

In all other runs, a mixture of fayalite, silicic acid and aluminium hydroxide is used.

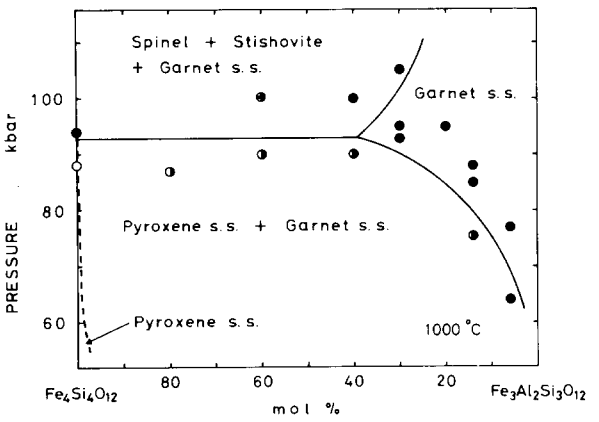

Fig. 6. Phase relationships in the system $Fe_4Si_4O_{12}$–$Fe_3Al_2Si_3O_{12}$ at pressures up to 105 kbar and at 1000°C. The pyroxene solvus is estimated from the high-pressure synthesis of aluminous ferrosilite, $FeSiO_3$·2.5wt.%Al_2O_3.

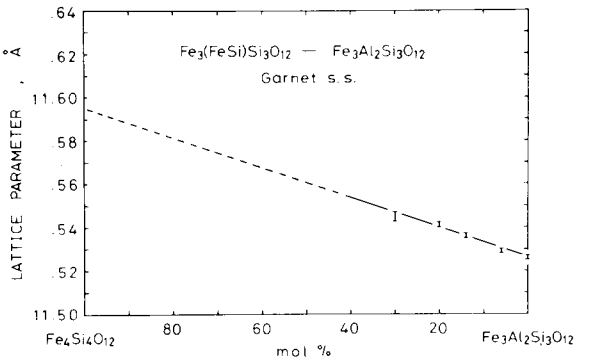

Fig. 7. Lattice parameter vs. composition of the homogeneous $Fe_4Si_4O_{12}$–$Fe_3Al_2Si_3O_{12}$ garnet solid solutions.

relationships at 1,000°C in the pressure range from 60 to 105 kbar are shown in Fig.6. The stability field of the garnet solid solution changes with pressure in a way similar to the $Mg_4Si_4O_{12}$–$Mg_3Al_2Si_3O_{12}$ system. The field expands to the $Fe_4Si_4O_{12}$-rich side up to 93 kbar and above that pressure it contracts to the $Fe_3Al_2Si_3O_{12}$-rich side. The transient pressure from expansion to contraction is just the same as that of the decomposition of clinoferrosilite to spinel (γ-Fe_2SiO_4) plus stishovite, determined by Akimoto and Syono (1970). In Fig. 6 a narrow single-phase field of pyroxene solid solution is also shown. Although the boundary curve of the field is tentatively assumed, the presence of pyroxene dissolving some amount of Al_2O_3 in the system $Fe_4Si_4O_{12}$–$Fe_3Al_2Si_3O_{12}$ has been demonstrated in the present study. At the composition 90%$Fe_4Si_4O_{12}$·10%$Fe_3Al_2Si_3O_{12}$ (mol%), an almost single-phase orthopyroxene was synthesized at 30 kbar and 1,200°C using a powder mixture of fayalite, α-quartz and corundum as starting materials (run No. 904 in Table V). A very small amount of garnet coexisting with the orthopyroxene was detected only by observation under the microscope. The lattice parameters and unit-cell volume of the orthopyroxene were determined as a = 18.422(3) Å, b = 9.056(2) Å, c = 5.230(2) Å, and V = 872.5(4) Å^3 using ten diffraction lines. These values are considerably smaller than those of orthoferrosilite: a = 18.436(2) Å, b = 9.072(1) Å, c = 5.243(2) Å, and V = 876.9(5) Å^3 (Matsui et al., 1968).

The chemical composition of the homogeneous garnet solid solution was determined by an electron microprobe analyser and the result is shown in Table II. It is confirmed that the garnet maintains the composition of the starting material in the system $Fe_4Si_4O_{12}$–$Fe_3Al_2Si_3O_{12}$. The solubility limit of $Fe_4Si_4O_{12}$ in $Fe_3Al_2Si_3O_{12}$ garnet at 1,000°C is about 40 mol%, which is smaller than 60 mol% of $Mg_4Si_4O_{12}$ in the system $Mg_4Si_4O_{12}$–$Mg_3Al_2Si_3O_{12}$. By comparing the experimental results obtained for the same composition and pressure at different temperatures (runs No. 3010 and 308 in Table V), it may be concluded that the garnet solid-solution solvus shifts to higher pressures with increasing temperature. This positive dP/dT value of the garnet solvus is quite similar to the system $Mg_4Si_4O_{12}$–$Mg_3Al_2Si_3O_{12}$.

In Fig. 7 a plot of lattice parameter vs. composition of the homogeneous garnet solid solution is shown. The lattice parameter increases almost linearly, from pure $Fe_3Al_2Si_3O_{12}$ almandine to the solubility limit, with an increasing amount of the $Fe_4Si_4O_{12}$ component. Present determination of the cell parameter of the synthetic almandine, 11.526(1) Å, is in close agreement with that reported by Skinner (1956). For the virtual garnet end-member, $Fe_4Si_4O_{12}$, a cell parameter of 11.595 Å is obtained by linear extrapolation. The density so estimated is 4.50 g/cm^3. This value is 12.8% greater than that of clinoferrosilite and is 4.7% smaller than that of a mixture of spinel (γ-Fe_2SiO_4) and stishovite in the same composition. The density and density increase which accom-

TABLE VI

Density of high-pressure phases in $MgSiO_3$ and $FeSiO_3$, and density increase which accompanies the phase transformations

Phase	Density (g/cm^3)	Density increase (%)	Ref.
$MgSiO_3$:			
Cpx	3.21	9.7 (Cpx → Gar)	(1)
Gar	3.52	4.5 (Gar → β + St)	(2)
β + St	3.68	1.6 (β + St → γ + St)	(3)
γ + St	3.74		(4)
$FeSiO_3$:			
Cpx	3.99	12.8 (Cpx → Gar)	(5)
Gar	4.50	4.7 (Gar → γ + St)	(6)
γ + St	4.71		(7)

Cpx = clinopyroxene; Gar = garnet; β = modified spinel; γ = spinel; St = stishovite.

References:

(1) = Stephenson et al. (1966).

(2) = present study. The extrapolated lattice parameter of virtual garnet of $Mg_4Si_4O_{12}$.

(3) β = Akimoto et al. (1976a); St = Akimoto and Syono (1969).

(4) γ = Ito et al. (1974).

(5) = Syono et al. (1971).

(6) = present study. The extrapolated lattice parameter of virtual garnet of $Fe_4Si_4O_{12}$.

(7) γ = Akimoto et al. (1965).

panies these transformations in $MgSiO_3$ and $FeSiO_3$ are summarized in Table VI. The density increase in the clinopyroxene–virtual garnet transformation in $MgSiO_3$ is a little smaller than in $FeSiO_3$. The density increase in $FeSiO_3$ is almost identical to the value, 13.1%, found for the clinopyroxene–tetragonal garnet transformation in $MnSiO_3$ (Akimoto and Syono, 1972).

Although X-ray powder diffraction patterns indicate that all the garnet solid solutions in the system $Fe_4Si_4O_{12}$–$Fe_3Al_2Si_3O_{12}$ have a cubic symmetry, the garnet, particularly containing more than 14 mol% of the $Fe_4Si_4O_{12}$ component, shows a slight birefringence under the microscope. This suggests that the exact symmetry of the garnet is lower than cubic. Garnet-like structures with the tetragonal unit cell have already been discovered in $CaGeO_3$, $CdGeO_3$ and $MnSiO_3$ (Ringwood and Seabrook, 1963; Ringwood and Major, 1967; Akimoto and Syono, 1972). Prewitt and Sleight (1969) analysed in detail the structure of $CdGeO_3$ and $CaGeO_3$ and established the ordering of Cd^{2+}, or Ca^{2+} and Ge^{4+}, in octahedral sites which causes the tetragonal distortion in the structure. Therefore, it may be expected that the ordered arrangement of Fe^{2+}, Si^{4+} and Al^{3+} in the octahedral sites takes place in the garnet solid solutions of the system $Fe_4Si_4O_{12}$–$Fe_3Al_2Si_3O_{12}$. In the garnet solid solutions of the system $Mg_4Si_4O_{12}$–$Mg_3Al_2Si_3O_{12}$, however, a disordering of Mg^{2+}, Si^{4+} and Al^{3+} in the octahedral sites is expected, because all the garnet solid solutions in the system are optically isotropic and have a cubic symmetry.

3.3. Geophysical implications

In Fig.8, a preliminary phase diagram at 1,200°C in the system $Mg_4Si_4O_{12}$–$Mg_3Al_2Si_3O_{12}$ is shown together with the diagram at 1,000°C. The isothermal section at 1,200°C is constructed with the aid of Figs. 2 and 5. To make the diagram more complete, two independent experimental data on the modified spinel (β)–spinel (γ) phase boundary in Mg_2SiO_4 (Kawada, 1977) and on the Al_2O_3 solubility limit in orthoenstatite coexisting with pyrope (MacGregor, 1974) are also used. It is known from Figs. 6 and 8 that the

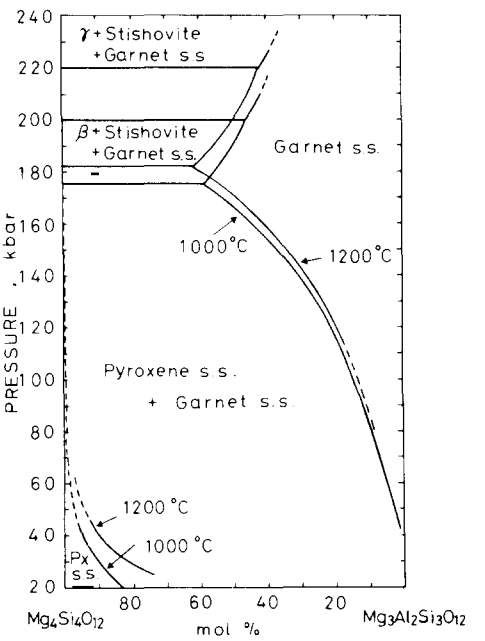

Fig. 8. Phase transformation diagram in the system $Mg_4Si_4O_{12}$–$Mg_3Al_2Si_3O_{12}$.

possible modes of transformation of pyroxenes in the mantle depend on the ratio of R_2O_3 (= Al_2O_3 + Cr_2O_3 + Fe_2O_3) to simple pyroxene components ($MgSiO_3$, $FeSiO_3$ and $CaSiO_3$). If we assume the pyrolite model for the mantle material according to Ringwood (1966), R_2O_3 amounts to about 10 wt.% of simple pyroxene components. It is further assumed in the following discussion that transformations of pyroxenes with 10% R_2O_3 can be approximated by those of a simple composition of $MgSiO_3 \cdot 10\%Al_2O_3$, which corresponds to the composition of $60\%Mg_4Si_4O_{12} \cdot 40\%Mg_3Al_2Si_3O_{12}$ (mol%). From the experimental results shown in Fig.8, the stable mineral assemblage in the upper mantle at depths shallower than about 150 km is expected to be pyroxene dissolving small amounts of Al_2O_3 and garnet with approximately pyrope composition. This is consistent with extensive petrological observations of ultramafic inclusions derived from the upper mantle. Fig.8 also indicates that the solubility of the pyroxene component in garnet increases gradually with increasing depth. This suggests that an appreciable amount of increase in the atomic number of Si for 12 oxygen atoms over the ideal value of 3 will be observed for garnet equilibrated with pyroxenes at depths greater than about 150 km. Chemical analyses of a number of garnets in South African kimberlites indicate that the atomic number of Si is in the range from 2.98 to 3.04 (Boyd and Nixon, 1972; Boyd, 1974). Considering the accuracy of the chemical analyses, no positive evidence for the solid solubility of a pyroxene component into these garnets was found in such a data survey. This implies that these garnets were possibly in equilibrium in the upper mantle at depths not greater than about 150 km. Since the garnets at greater depths are expected to dissolve a higher amount of the pyroxene component, the occurrence of garnets with more than 3 Si per formula unit is very probable in rocks derived from the upper mantle at depths around 200 km.

It is further expected from Fig.8 that at greater depths the pyroxene–garnet assemblage will become unstable and transform completely to a homogeneous garnet solid solution. Based on Fig.8, zero-pressure densities for the composition of $60\%Mg_4Si_4O_{12} \cdot 40\%Mg_3Al_2Si_3O_{12}$ (mol%) at varying pressures or depths are calculated and shown in Fig.9. In this calculation, the pressure distribution within the earth

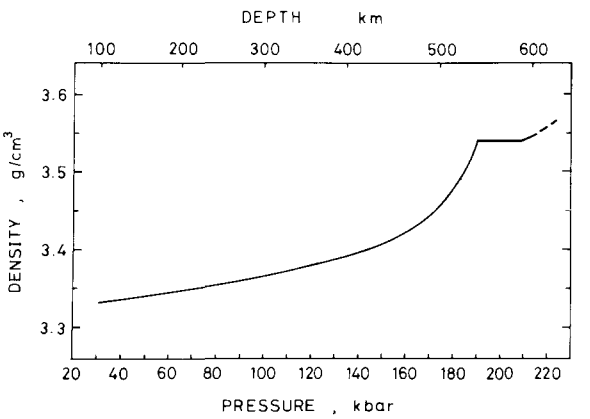

Fig. 9. Zero-pressure density vs. depth (pressure) in $60\%[Mg_4Si_4O_{12}] \cdot 40\%[Mg_3Al_2Si_3O_{12}]$ (mol%).

according to Bullen's A model (Bullen, 1963) and a temperature–depth curve, smoothly extrapolated using the continental geotherm by Clark and Ringwood (1964), are adopted. As is seen in Fig.9, the density increases slowly with increasing depth, up to 450 km, by dissolving a small amount of pyroxene component in the pyrope garnet. In the range of depths from about 450 to 540 km, a high gradient of the density increase appears. This corresponds to a rapid expansion of the homogeneous garnet field. The single-phase garnet solid solution is stable at depths from about 540 to 590 km, below which the garnet solid solution decomposes into the three-phase mixture composed of modified spinel (β), stishovite and garnet containing a lower pyroxene component. Although the total density increase from 100 to 540 km is 6.2%, the rather rapid increase from 450 to 540 km amounts to 3.7%. Since fairly large amounts of $(Mg,Fe)_2SiO_4$ orthosilicates are present in the upper mantle in addition to pyroxene and garnet, the density change associated with the high solubility of the pyroxene component into garnet at depths between 450 and 540 km becomes smaller than the above-estimated value and is calculated to be 1.6% for the pyrolite mantle.

Recent laboratory measurement of the ultrasonic wave velocities for the high-pressure polymorphs of $CaGeO_3$ and $CdGeO_3$ indicates that the jump in P-wave velocity which accompanies the transformation from the pyroxene-related structure to the garnet structure is 1.2–1.5 times larger than expected by the density jump (Liebermann, 1974). Therefore, about

2% increase in P-wave velocity at depths between 450 and 540 km is likely to be caused by the 1.6% density increase in the pyrolite mantle. Recent analyses of the seismic body-wave propagation have revealed that an abrupt change in the slope of the velocity–depth curve occurs between approximately 450 and 550 km (Helmberger and Wiggins, 1971; Helmberger and Engen, 1974; Simpson et al., 1974; Fukao, 1977). Evidence for the discontinuity at ca. 500 km has also been obtained from the reflection of p′p′ seismic waves (Whitcomb and Anderson, 1970). This minor discontinuity in the mantle transition zone has been attributed to the modified spinel (β)–spinel (γ) transformation in the system Mg_2SiO_4–Fe_2SiO_4 (Whitcomb and Anderson, 1970; Burdick and Anderson, 1975; Ringwood, 1975; Akimoto et al., 1976a, b). The experimental results in the present study suggest that the most effective velocity increase due to the pyroxene–garnet transformation can be expected at depths around 500 km. This leads to the conclusion that the minor discontinuity around 500 km in the seismic wave-velocity structure may be due to the superposition effect of these two-phase transformations; the β–γ transformation in $(Mg,Fe)_2SiO_4$ and the pyroxene–garnet transformation. Very recently, Anderson (1976) has attempted to infer the mineral assemblages down to 800 km by comparing elastic moduli data of silicates and oxides with seismic data. He pointed out that in the region between 500 and 600 km the mineral assemblage was expected to be modified spinel (β) or spinel (γ) plus garnet rather than γ plus stishovite. Figs. 8 and 9 suggest that only a very small amount (if any) of stishovite can be equilibrated with garnet solid solution at depths below 590 km. Accordingly, substantial support for Anderson's conclusion is afforded by the present phase equilibrium investigation on the system $Mg_4Si_4O_{12}$–$Mg_3Al_2Si_3O_{12}$.

In the above discussion, transformations of the pyroxene–garnet assemblage in the mantle are approximated by those of a specific composition in the simple system $Mg_4Si_4O_{12}$–$Mg_3Al_2Si_3O_{12}$. The presence of other cations, such as Fe^{2+} and Ca^{2+}, capable of substituting Mg^{2+} must be considered for the actual mantle. By comparing Fig.3 with Fig.6, it is very probable that the presence of Fe^{2+} remarkably reduces the pyroxene–garnet transformation pressure in the mantle. If we consider the mineralogic distribution of Mg^{2+} and Fe^{2+} in the mantle transition zone, however, it turns out that the presence of Fe^{2+} may not result in a great change in the above conclusion. In previous investigations on the chemical equilibrium partitioning of Mg^{2+} and Fe^{2+} among $(Mg,Fe)_2SiO_4$ olivine or spinel, $(Mg,Fe)SiO_3$ pyroxene and $(Mg,Fe)_3Al_2Si_3O_{12}$ garnet, relative enrichment of Fe^{2+} in the $(Mg,Fe)_2SiO_4$ spinel solid solutions was established at the pressure–temperature condition corresponding to the mantle transition zone (Nishizawa and Akimoto, 1973; Akimoto et al., 1976b). It is clear from the present study that the main part of the pyroxene–garnet transformation occurs at pressures a little higher than the olivine (α)–modified spinel (β) transformation pressure in $(Mg,Fe)_2SiO_4$. Thus, it is likely that the pyroxene–garnet assemblage relevant to the main part of the pyroxene–garnet transformation is rather depleted in Fe^{2+}: the most probable value for the $Mg^{2+}/(Mg^{2+} + Fe^{2+})$ ratio in the homogeneous garnet solid solution will be around 0.95. From these considerations, the present simple argument based on the $Mg_4Si_4O_{12}$–$Mg_3Al_2Si_3O_{12}$ system may be taken as a first approximation.

Acknowledgments

The authors wish to thank Dr. K. Kawada of the Institute for Solid State Physics, University of Tokyo for his valuable advice in operating the double-staged cubic-octahedral-anvil apparatus developed by him. They are also grateful to Dr. H. Takei, Tohoku University for providing the starting materials of glass and to Dr. E. Ito, Okayama University and Dr. T. Mori, Australian National University for their helpful comments and discussions. This work was supported under a special grant from the Ministry of Education for the Japanese Geodynamics Project.

References

Akimoto, S. and Fujisawa, H., 1965. Demonstration of electrical conductivity jump produced by the olivine–spinel transition. J. Geophys. Res., 70: 443–450.

Akimoto, S. and Syono, Y., 1969. Coesite–stishovite transition. J. Geophys. Res., 74: 1653–1659.

Akimoto, S. and Syono, Y., 1970. High pressure decomposition of the system $FeSiO_3$–$MgSiO_3$. Phys. Earth Planet. Inter., 3: 186–188.

Akimoto, S. and Syono, Y., 1972. High pressure transformations in $MnSiO_3$. Am. Mineral., 57: 76–84.

Akimoto, S., Fujisawa, H. and Katsura, T., 1965. The olivine–spinel transition in Fe_2SiO_4 and Ni_2SiO_4. J. Geophys. Res., 70: 1969–1977.

Akimoto, S., Yagi, T., Ida, Y., Inoue, K. and Sato, Y., 1975. High-pressure X-ray diffraction study on barium up to 130 kbar. High Temp.–High Pressures, 7: 287–294.

Akimoto, S., Matsui, Y. and Syono, Y., 1976a. High pressure crystal chemistry of orthosilicates and formation of the mantle transition zone. In: R.G.J. Strens (Editor), The Physics and Chemistry of Minerals and Rocks, Wiley, London, pp. 327–363.

Akimoto, S., Akaogi, M., Kawada, K. and Nishizawa, O., 1976b. Mineralogic distribution of iron in the upper half of the transition zone in the earth's mantle. In: G.H. Sutton, M.H. Manghnani and R. Moberly (Editors), The Geophysics of the Pacific Ocean Basin and Its Margin, Am. Geophys. Union, Geophys. Monogr., 19: 399–405.

Akimoto, S., Yagi, T. and Inoue, K., 1977. High temperature–pressure phase boundaries in silicate systems using in situ X-ray diffraction. In: M.H. Manghnani and S. Akimoto (Editors), High-pressure Research: Applications in Geophysics, Academic Press, New York, N.Y., pp. 585–602.

Anderson, D.L., 1976. The 650 km mantle discontinuity. Geophys. Res. Lett., 3: 347–349.

Bence, A.E. and Albee, A.L., 1968. Empirical correction factors for the electron microanalysis of silicates and oxides. J. Geol., 76: 382–403.

Boyd, F.R., 1974. Ultramafic nodules from the Frank Smith kimberlite pipe, South Africa. Carnegie Inst. Washington Yearb., 73: 285–294.

Boyd, F.R. and England, J.L., 1959. Pyrope. Carnegie Inst. Washington Yearb., 58: 83–87.

Boyd, F.R. and England, J.L., 1964. The system enstatite–pyrope. Carnegie Inst. Washington Yearb., 63: 157–161.

Boyd, F.P. and Nixon, P.H., 1972. Ultramafic nodules from the Thaba Putsoa kimberlite pipe. Carnegie Inst. Washington Yearb., 71: 362–373.

Bullen, K.E., 1963. An Introduction to the Theory of Seismology. Cambridge University Press, London, 3rd ed., 381 pp.

Burdick, L.J. and Anderson, D.L., 1975. Interpretation of velocity profiles of the mantle. J. Geophys. Res., 80: 1070–1074.

Clark, S.P. and Ringwood, A.E., 1964. Density distribution and constitution of the mantle. Rev. Geophys., 2: 35–88.

Fukao, Y., 1977. Upper mantle P-structure and 650 km discontinuity. In: M.H. Manghnani and S. Akimoto (Editors), High-Pressure Research: Applications in Geophysics, Academic Press, New York, N.Y., pp. 151–161.

Helmberger, D.V. and Engen, G.R., 1974. Upper mantle shear structure. J. Geophys. Res., 79: 4017–4028.

Helmberger, D.V. and Wiggins, R.A., 1971. Upper mantle structure of midwestern United States. J. Geophys. Res., 76: 3229–3245.

Inoue, K., 1975. Development of high temperature and high pressure X-ray diffraction apparatus with energy dispersive technique and its geophysical applications. Ph.D. Thesis, University of Tokyo, Tokyo.

Ito, E., 1977a. The absence of oxide mixture in high pressure phases of Mg-silicates. Geophys. Res. Lett., 4: 72–74.

Ito, E., 1977b. Ultrahigh pressure studies of geophysically important silicates. Ph.D. Thesis, University of Tokyo, Tokyo.

Ito, E., Matsumoto, T., Suito, K. and Kawai, N., 1972. High pressure break-down of enstatite, Proc. Jpn. Acad., 48: 412–415.

Ito, E., Matsui, Y., Suito, K. and Kawai, N., 1974. Synthesis of γ-Mg_2SiO_4. Phys. Earth Planet. Inter., 8: 342–344.

Kawada, K., 1977. The system Mg_2SiO_4–Fe_2SiO_4 at high pressures and temperatures and the earth's interior. Ph.D. Thesis, University of Tokyo, Tokyo.

Kawai, N. and Endo, S., 1970. The generation of ultrahigh hydrostatic pressures by a split sphere apparatus. Rev. Sci. Instrum., 41: 1178–1181.

Kawai, N., Tachimori, M. and Ito, E., 1974. A high pressure hexagonal form of $MgSiO_3$. Proc. Jpn. Acad., 50: 378–380.

Liebermann, R.C., 1974. Elasticity of pyroxene–garnet and pyroxene–ilmenite phase transformations in germanates. Phys. Earth Planet. Inter. 8: 361–374.

Liu, L., 1974. Silicate perovskite from phase transformations of pyrope–garnet at high pressure and temperature. Geophys. Res. Lett., 1: 277–280.

Liu, L., 1975. Post-oxide phases of forsterite and enstatite. Geophys. Res. Lett., 2: 417–419.

Liu, L., 1976a. Orthorhombic perovskite phases observed in olivine, pyroxene and garnet at high pressures and temperatures. Phys. Earth Planet. Inter., 11: 289–298.

Liu, L., 1976b. The high-pressure phases of $MgSiO_3$. Earth Planet. Sci. Lett., 31: 200–208.

MacGregor, I.D., 1974. The system MgO–Al_2O_3–SiO_2: Solubility of Al_2O_3 in enstatite for spinel and garnet peridotite compositions. Am. Mineral., 59: 110–119.

Matsui, Y., Syono, Y., Akimoto, S. and Kitayama, K., 1968. Unit cell dimensions of some synthetic orthopyroxene group solid solutions. Geochem. J., 2: 61–70.

Ming, L. and Bassett, W.A., 1975. High pressure phase transformations in the system of $MgSiO_3$–$FeSiO_3$. Earth Planet. Sci. Lett., 27: 85–89.

Nakamura, Y. and Kushiro, I., 1970. Compositional relations of coexisting orthopyroxene, pigeonite and augite in a tholeiitic andesite from Hakone Volcano. Contrib. Mineral. Petrol., 26: 265–275.

Nishizawa, O. and Akimoto, S., 1973. Partition of magnesium and iron between olivine and spinel and between pyroxene and spinel. Contrib. Mineral. Petrol., 41: 217–230.

Prewitt, C.T. and Sleight, A.W., 1969. Garnet-like structures of high-pressure cadmium germanate and calcium germanate. Science, 163: 386–387.

Ringwood, A.E., 1966. The chemical composition and origin of the earth. In: P.M. Hurley (Editor), Advances in Earth Science, M.I.T. Press, Cambridge, Mass., pp. 287–356.

Ringwood, A.E., 1967. The pyroxene–garnet transformation in the earth's mantle. Earth Planet. Sci. Lett., 2: 255–263.

Ringwood, A.E., 1970. Phase transformations and constitution of the mantle. Phys. Earth Planet. Inter., 3: 109–155.
Ringwood, A.E., 1975. Composition and Petrology of the Earth's Mantle. McGraw-Hill, New York, N.Y., 618 pp.
Ringwood, A.E. and Major, A., 1966. High pressure transformations in pyroxenes. Earth Planet. Sci. Lett., 1: 351–357.
Ringwood, A.E. and Major, A., 1967. Some high-pressure transformations of geophysical significance. Earth Planet. Sci. Lett., 2: 106–110.
Ringwood, A.E. and Major, A., 1968a. High pressure transformations in pyroxenes, II. Earth Planet. Sci. Lett., 5: 76–78.
Ringwood, A.E. and Major, A., 1968b. Apparatus for phase transformation studies at high pressures and temperatures. Phys. Earth Planet. Inter., 1: 164–168.
Ringwood, A.E. and Seabrook, M., 1963. High pressure phase transformations in germanate pyroxenes and related compounds. J. Geophys. Res., 68: 4601–4609.
Simpson, D.W., Mereu, R.F. and King, D.W., 1974. An array study of P-wave velocities in the upper mantle transition zone beneath northeastern Australia. Bull. Seismol. Soc. Am., 64: 1757–1788.
Skinner, B.J., 1956. Physical properties of end-members of the garnet group. Am. Mineral., 41: 428–436.
Skinner, B.J. and Boyd, F.R., 1964. Aluminous enstatite. Carnegie Inst. Washington Yearb., 63: 163–165.
Smith, J.V. and Mason, B., 1970. Pyroxene–garnet transformation in Coorara meteorite. Science, 168: 832–833.
Stephenson, D.A., Sclar, C.B. and Smith, J.V., 1966. Unit cell volumes of synthetic orthoenstatite and low clinoenstatite. Mineral. Mag., 35: 838–846.
Syono, Y., Akimoto, S. and Matsui, Y., 1971. High pressure transformations in zinc silicates. J. Solid State Chem., 3: 369–380.
Whitcomb, J.H. and Anderson, D.L., 1970. Reflection of P′P′ seismic waves from discontinuities in the mantle. J. Geophys. Res., 75: 5713–5728.
Yagi, T. and Akimoto, S., 1976a. Direct determination of coesite–stishovite transition by in situ X-ray measurements. Tectonophysics, 35: 259–270.
Yagi, T. and Akimoto, S., 1976b. Pressure fixed points between 100 and 200 kbar based on the compression of NaCl. J. Appl. Phys., 47: 3350–3354.
Yagi, T. and Akimoto, S., 1977. Pressure calibration above 100 kbar based on the NaCl internal standard. In: M.H. Manghnani and S. Akimoto (Editors), High-Pressure Research: Applications in Geophysics, Academic Press, New York, N.Y., pp. 573–583.

Note added in proof

After completion of the present paper, Lin-Gun Liu has sent us a preprint of his paper entitled: "The system enstatite–pyrope at high pressures and temperatures" which was published in *Earth and Planetary Science Letters* (Vol. 36, No. 1, pp. 237–245). The proposed phase diagram for the pyroxene–garnet transformation in the system is in substantial agreement with the present results. Further, he reports that the garnet phase with compositions of $(Mg_4Si_4O_{12})_x(Mg_3Al_2Si_3O_{12})_{1-x}$ ($x = 0.6, 0.8$) transforms to the ilmenite structure and then to the orthorhombic perovskite structure in the pressure range 220–280 kbar at about 1,000°C.